Measurements of deformation, schlieren and forces on an OAT15A airfoil at pre-buffet and buffet conditions

Measurements of deformation, schlieren and forces on an OAT15A airfoil at pre-buffet and buffet conditions

Alessandro Accorinti[1], Tim Baur[1], Sven Scharnowski[1], Johannes Knebusch[2], Johannes Dillinger[2], Yves Govers[2], Jens Nitzsche[2], Christian J. Kähler[1]

[1]Institut für Strömungsmechanik und Aerodynamik, Universität der Bundeswehr München, Neubiberg, Germany

[2] Institut für Aeroelastik, Deutsches Zentrum für Luft- und Raumfahrt e.V. (DLR), Göttingen, Germany

alessandro.accorinti@unibw.de

Abstract. Self-sustained shock wave oscillations on airfoils, commonly defined as shock buffet, can occur under certain combinations of transonic Mach number and angle of attack due to the interaction between the shock and the separated boundary layer. To help understanding buffet physics, a rigid supercritical wing model (OAT15A) was investigated in pre-buffet and buffet conditions using a combined application of BOS (Background Oriented Schlieren), deformation and force measurements. From the observation via BOS of the change of the shock location and the extent of the boundary layer separation with the AoA (angle of attack), the transition from stable shock to buffet was detected. A comparison with other research groups at supposedly similar aerodynamic conditions highlighted a great disparity among them in terms of buffet onset, amplitudes of buffet oscillations, and flow development (motion of the mean shock location with the AoA) after the onset. The average and rms (root mean square) of the surface displacement were computed together with the effective geometric AoA, taking into account the static torsional deformation of the model and its support. Moreover, the spectra of the balance and deformation data showed the same buffet peak as in the BOS spectrum, indicating a coupling between structure and flow, which increased with the AoA.

1. Introduction

The flow instability known as shock buffet ensues due to the interaction between the shock and the separated boundary layer on the upper surface of a wing under certain combinations of transonic Mach number and AoA (angle of attack). It brings about self-sustained shock oscillations, whose frequency is normally in the same order of magnitude of low structural Eigenfrequencies, which can lead to FSI (fluid-structure interaction) and reduction of the aircraft performances. There are already several existing models trying to explain the physics behind buffet. One of them is the one proposed by [1] and consists of a feedback loop between the shock and the TE (trailing edge). This model consents to fairly predict the buffet frequency but only for specific types of geometry. Another approach is the one introduced by [2], which allows for predicting the buffet onset and its frequency and consists in a

global mode decomposition of the RANS (Reynolds-averaged Navier–Stokes) equations. By doing that, it is possible to compute the aerodynamic modes and to track down the unstable one, which is responsible for the phase-locked modulation between the shock and the boundary layer. However, several aspects of this complex phenomenon are still to be thoroughly understood and, with this regard, a close collaboration between numerics and experiments is of crucial importance.

2. Description of the model and its support

The model and its support are depicted in Figure 1:

- The **CFRP-wing (blue)**, for which a standard supercritical profile (OAT15A) was selected, is rigidly mounted in the wind tunnel.
- The **steel shaft (blue)** transfers the aerodynamic loads to the force balances, which are placed in the plenum chamber.
- The **moment-free needle bearing (cyan) with mount (brown)** takes up and transfers loads (only forces) from the shaft to the 3-component force balance and allows for a friction-reduced rotation of the shaft.
- The **3-component force balance (red) with mount (grey)** measures the aerodynamic forces.
- The **moment-lever-arm (purple)** serves multiple functions: not only plays it the role of an adjustable torsional spring (currently, the stiffness is set to a high value in order to prevent the pitching degree of freedom.) but it also transfers the aerodynamic moment to the 1-component force.
- The **1-component force (green)** measures the aerodynamic moment as a force. By changing the height at which it is fixed to the lever arm, it is possible to set different spring stiffness values.

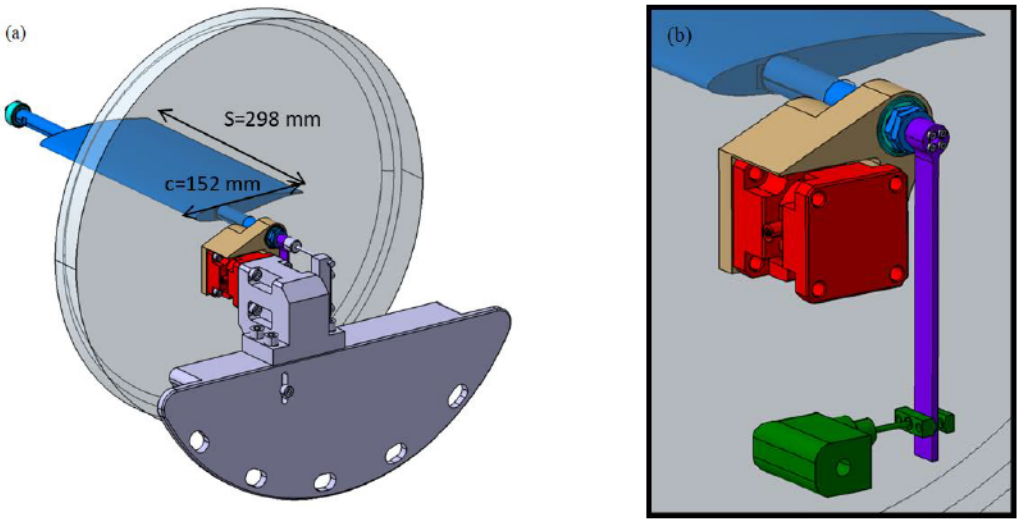

Figure 1. (a) Wing model and its support; (b) Focus of the support of the model.

3. Description of the facility and the measurement techniques

The TWM (Trisonic wind tunnel of Munich) facility is a blow-down wind tunnel with a 300 mm wide and 680 mm high test section ideally suited for profile measurements. In the transonic regime, an operation time of about 100 seconds can be achieved up to 6 times per day. Its test section is illustrated in Figure 2. A random speckle pattern was applied to the model upper surface in order to optimize the correlation-based deformation measurements (Figure 2 (b)). Previously, a regular dot pattern showed a

lack of correlation results. It remained below the random speckle pattern as it served the purpose of tripping the boundary layer at the position of 7% of the chord (upper and lower surface). In addition, a random reference pattern was applied to the force balance mount (brown in Figure 1) and was used to separate the model and the camera motion and correct the recorded images for the latter. The light coming from two UV LEDs on top of the test section (Figure 2 (d)) is scattered by the model and reaches at each side of the test section a PCO Dimax HS4 camera through a mirror (Figure 2 (e)). Making use of a preceding coplanar stereo camera calibration throughout the whole test section, a correlation-based surface reconstruction was performed for every time instant. As a result, the 3-D components of the surface displacement could be obtained. In order to perform BOS measurements from the side, a random point-like pattern, whose points are 2 pixels in diameter (0.5 mm) and whose point density is slightly above 40%, was installed in the background of the test section (Figure 2 (a) and (b)). The test section and the pattern are illuminated by a blue LED and recorded by a Phantom V2640 high-speed camera (Figure 2 (e)). Figure 2 (c) shows a wind-on BOS image with a shock above the model. The dark circular region is caused by high mechanical stresses in the window due to a hole needed for the model mounting. The force balances and several accelerometers placed on the moment arm complete the setup.

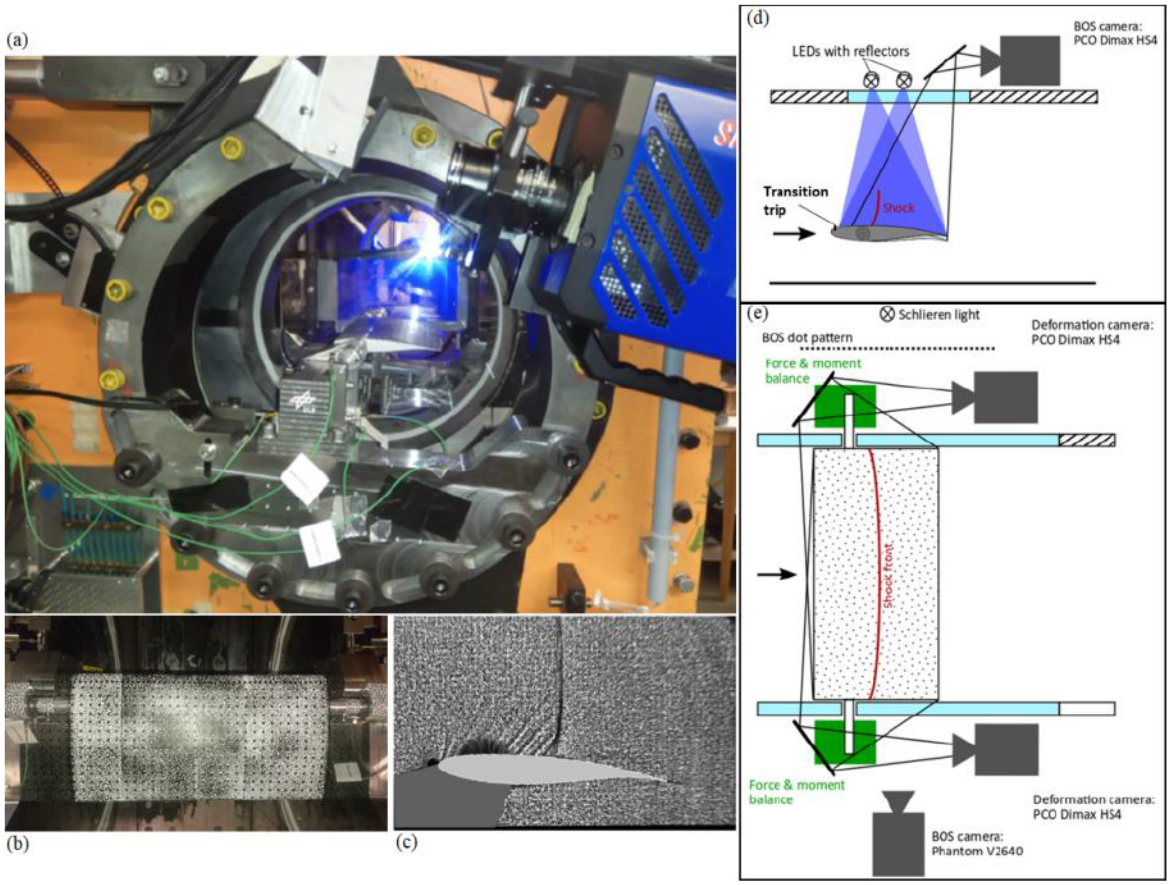

Figure 2. (a) TWM test section and instrumentation; (b) deformation pattern; (c) BOS pattern; (d) setup of BOS from the top; (e) setup of deformation and BOS from the side.

4. Presentation of the study case

To select AoA-Mach combinations particularly suited for the buffet investigation, some references already present in the literature were exploited. Figure 3 shows the results of several AoA-Mach steady solutions with the Spalart–Allmaras turbulence model provided by [3], where the shock location in chord percentages is colour-coded. The red dashed line represents the minimum AoA for each Mach number where the shock starts to move towards the LE (leading edge) with the increase of the AoA, which is a necessary condition for the shock buffet. Therefore, even though the numerical simulations are all stable (no buffet) due to the turbulence model, they still indicate the region above the red line as potentially interesting for the buffet investigation. A further reference was constituted by the work of [4], who found a fully developed buffet flow at Mach=0.73 and AoA=3.5°. This parameter combination (black star) was selected as design point and, in the attempt of recreating the same conditions in the TWM, several AoA sweeps were performed (black arrows). Afterwards, the analysis was narrowed down to the cases (circles) with the least difference with the results of [4] in terms of shock position before buffet onset, flow development (change of the mean shock position with the AoA) after buffet onset and buffet frequency. The focus of this paper is put on the M=0.74 case (red circles).

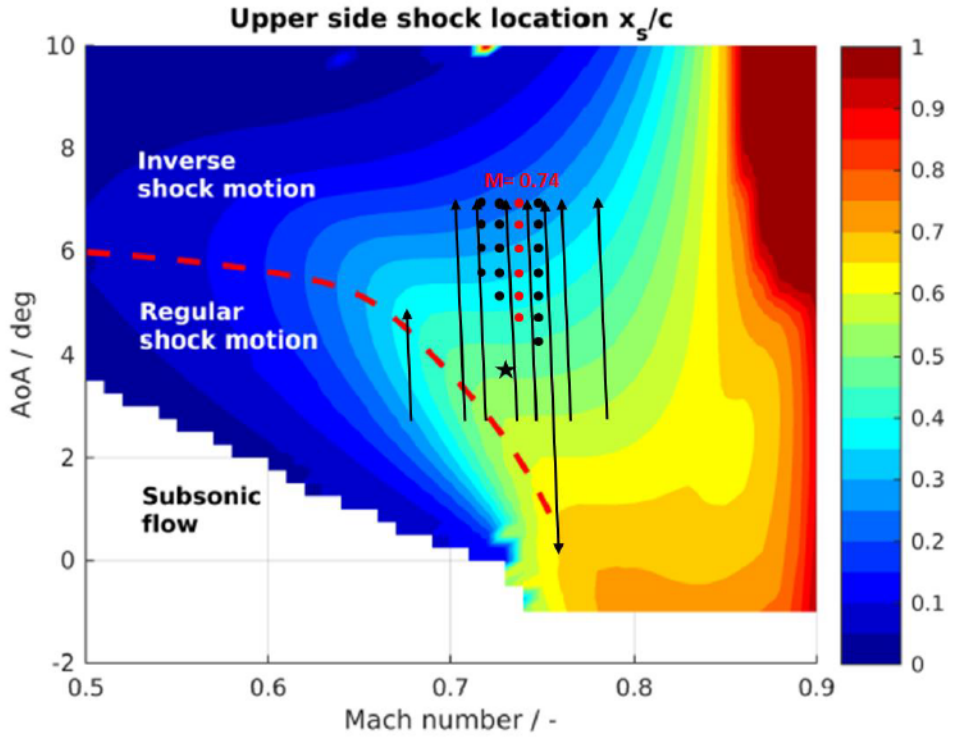

Figure 3. Colour-coded shock position in chord percentages for several AoA and Mach combinations from [3]. The black star refers to the combination investigated in [4], while the arrows and the circles to the ones investigated by the authors of this paper.

5. BOS results

Figure 4 shows the colour-coded displacement field in pixels, the result of the cross-correlation between wind off and wind on BOS images: positive displacements correspond to positive density gradients and negative displacements to negative ones. The size of the IA (interrogation area) in the cross-correlation was progressively reduced in a multi-pass calculation from 64×64 to 8×8 pixels. The black stars show every 10% of the chord and the red one the position of the rotational axis.

The line that connects the black circles displays the instantaneous position of the shock that was computed for several normal distances to the surface, based on the location of the maximum of the signal. In Figure 5, instead, the mean (time-averaged) shock position is plotted together with the rms (root mean square) of the shock oscillations as a horizontal error bar. At an AoA of 5° and a distance of 10% of the chord from the upper surface, the shock seems relatively stable at 46% of the chord, and the boundary layer is still attached. Increasing the AoA to 6°, the mean shock position moves towards the LE (44% of the chord), that is the necessary condition for buffet onset is fulfilled. The boundary layer, moreover, looks partially separated. Finally, at AoA=7°, a developed buffet is observed with a mean shock position at 39% of the chord and a rms which is considerably higher than the one at 5°. Furthermore, the boundary layer is completely separated.

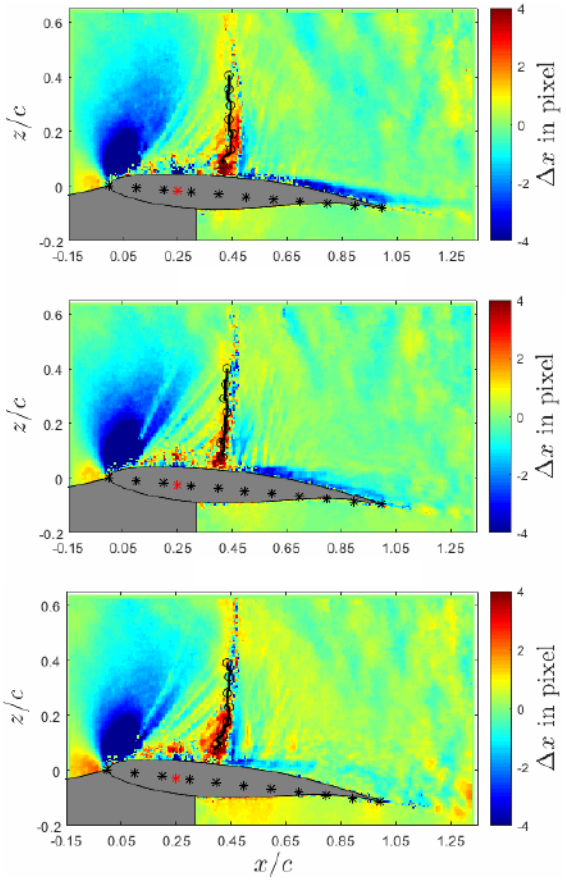

Figure 4. Colour-coded displacement field in pixels at M=0.74. From top to bottom AoA=5°, 6° and 7°.

6. Comparison with literature cases

In Figure 6, the shock position is plotted together with the maximum amplitude of its oscillations as error bar over the AoA for different research groups. The stars represent stable shocks (pre-buffet), the circles the buffet onset, and the triangles the mean shock location for oscillating shock waves (post-buffet onset). In black, the results of [4] are plotted, where the shock position is deduced from the pressure taps on the upper surface of a model characterized by an AR (aspect ratio) of 3.4. The Reynolds number is $Re_c=3\times10^6$ and the Mach number is M=0.73. The mean shock position before buffet onset is around 48% of the chord and then it progressively moves towards the LE after onset (3.1°), which satisfies the aforementioned necessary condition for buffet, with increasing oscillation amplitudes. In green, the results of the steady numerical solutions for a 2D profile of [3] are shown. The shock position is once again

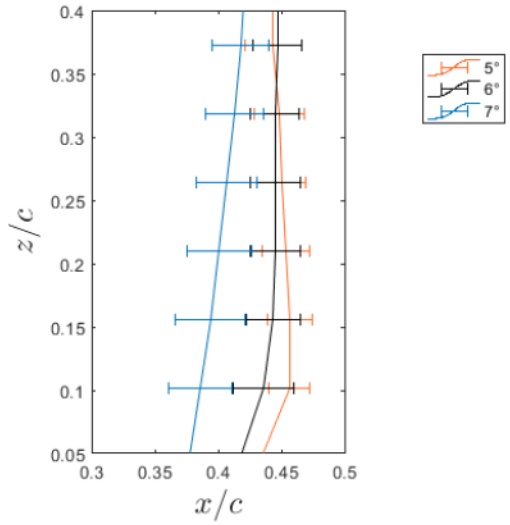

Figure 5. Mean shock position and shock oscillation rms at M=0.74.

extracted from the pressure values at the surface. The plotted values refer to $Re_c=3\times10^6$ and M=0.73. A similar position as the pre-buffet one shown by [4] is reached at a slightly higher AoA (3.75°). Even though all the solutions are steady, the flow development is similar to the buffet flows of [4]. In cyan, the data of [5] are shown: the shock position is deduced by Schlieren measurements at a vertical distance of 10% of the chord from the upper surface of a model characterized by an AR of 2.8. The Reynolds number is $Re_c=2.8\times10^6$, while the set Mach is 0.7 (0.73 according to the blockage corrections). Fully developed buffet flows are already present at around 2.5°, much earlier than [4]. Also, the mean shock position moves towards the TE instead of the LE with the increase of the AoA. In red, the results of the authors of this paper are depicted: the shock position is extracted from the BOS data at a normal distance to the upper surface of 10% of the chord. The Reynolds number is $Re_c=3\times10^6$ and the Mach number is M=0.74, while the AR is 2. Shock buffet occurs at an AoA of about 6°, which is significantly higher than [4]. The intensity of the oscillations is also clearly smaller and the flow development slower. This may be linked to the gap flow at the wind tunnel sidewalls, which could reduce the effective AoA, and will be therefore investigated in the future. All in all, great diversity among the research groups can be noticed, suggesting the influence of wind tunnel and model characteristics.

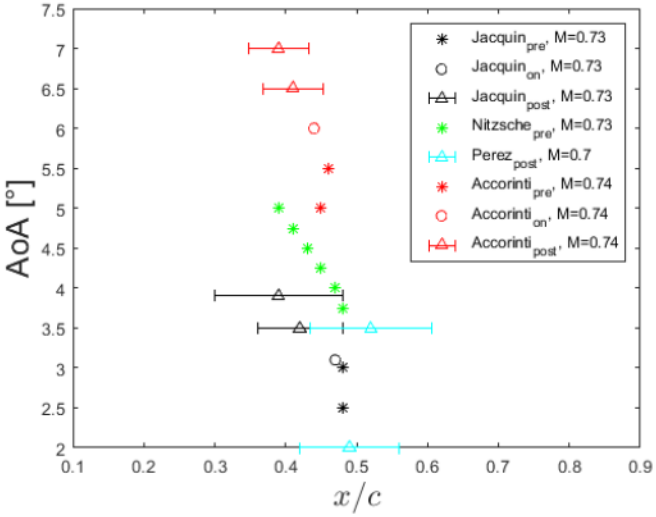

Figure 6. Mean shock position and shock oscillation amplitude over the AoA for several research groups.

7. Deformation results

Figure 7 illustrates the average surface vertical displacement of all the points on the upper surface of the model with respect to the wind-off conditions for one combination of Mach number and AoA. One can easily recognize that the points closer to the TE and the spanwise centre deform more than those close to the LE and the sidewall. In particular, focusing on the locations highlighted by the coloured arrows, it is possible to examine the deformation trend with the AoA (see Figure 8, top). Until AoA=5.5°, the mean vertical displacement tends to grow linearly and the rms of the oscillations to stay almost constant with the AoA. This uniform displacement of all points represents the static deformation of the partially flexible parts (mainly torsion of the shaft). At higher AoAs, instead, the mean displacement reaches a plateau and the rms of the oscillations soars, indicating that the interaction between the structure and the flow intensifies. Thanks to the deformation measurements, it was also possible to reconstruct the effective geometrical AoA, taking into account the static torsion of the model and its support (see Figure 8, bottom). The effective AoA is 0.5°-0.6° smaller than the one set in the TWM, which contributes to delay the buffet onset to higher AoAs.

8. Frequency analysis

Figure 9 shows the PSD (power spectral density) of the fluctuations of the vertical displacement of the point highlighted by the green arrow in Figure 7 measured by the deformation cameras (red), of the shock location computed via BOS (blue), and of the vertical force recorded by the 3D force balance (green). At an AoA of 5°, no clear peak can be seen for the BOS signal, indicating a stable shock,

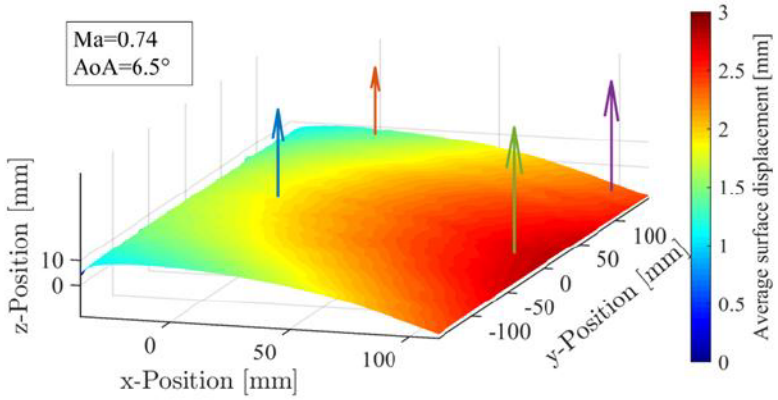

Figure 7. Average vertical displacement of the upper surface of the model with respect to reference wind-off conditions.

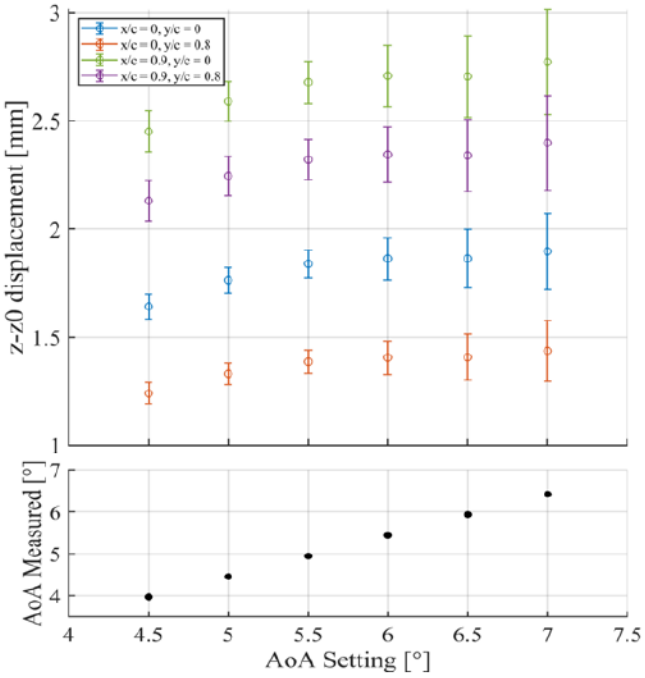

Figure 8. Top: Average vertical displacement of four points on the upper surface with respect to reference wind-off conditions over the set AoA; Bottom: Measured geometrical AoA over the set one.

while the first three structural Eigenfrequencies (respectively heave, pitch coupled with streamwise motion and pitch) are present in both deformation and balance data. Increasing the AoA to 6°, a peak appears in the BOS data around 92 Hz confirming that the buffet onset has already been reached. Simultaneously, a very similar peak is shown in the deformation and balance spectra, pointing out an interaction between the buffet and the heave mode. Finally, at 7°, the buffet peak moves towards higher frequencies (122 Hz) and increases in intensity, suggesting higher shock amplitudes. The structural oscillations also show the same peak, with a stronger fluid-structure interaction, while a broader peak region is shown in the balance data, probably due to the fact that the buffet and heave frequencies are getting very close to each other.

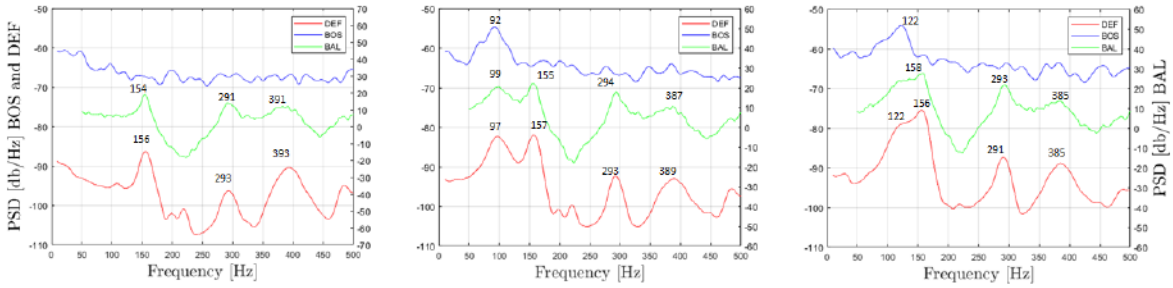

Figure 9. PSD of the frequency content of the deformation, BOS and balance data. From left to right: AoA=5°, 6° and 7°.

9. Conclusions

The buffet onset and the following development of the flow were characterized via BOS measurements. According to these results, the buffet onset occurred at significantly higher AoAs and with smaller amplitudes of the oscillations and slower flow development in comparison with [4]. Among the possible reasons, there is the influence of the gap flow at the wind tunnel sidewalls, which could reduce the effective AoA, and will be therefore investigated in the future. However, the results showed a significant difference among the research groups, suggesting that the wind tunnel and model characteristics may play a significant role in the characterization of the aerodynamic phenomena. Moreover, the 3D displacement field of the upper surface of the model was measured by the deformation cameras together with the effective geometric AoA, which takes into account the static deformation. The spectra of the balance and deformation data were computed, showing the same buffet peak as in the BOS spectrum, sign of the interaction between the heave structural mode and the flow, which increased with the AoA. In the near future, the pitching DOF will be released, by significantly reducing the corresponding Eigenfrequency from the current value of 380 to 90 Hz, which is very close to the computed buffet frequency, with the aim to generate a specific type of FSI between the two of them, namely Fluid Mode Flutter [3].

References

[1] Lee B H K 1990 Oscillatory shock motion caused by transonic shock boundary-layer interaction *AIAA J.* **28** 942–44.
[2] Crouch J D, Garbaruk A, Magidov D and Travin A 2009 Origin of transonic buffet on aerofoils *J. Fluid Mech.* **628** 357–69.
[3] Nitzsche J, Ringel L M, Kaiser C and Hennings H 2019 Fluid-mode flutter in plane transonic flows *International Forum on Aeroelasticity and Structural Dynamics IFASD*.
[4] Jacquin L, Molton P, Deck S, Maury B and Soulevant D 2009 Experimental study of shock oscillation over a transonic supercritical profile *AIAA J.* **47** 1985–94.
[5] Pérez R S 2017 On the unsteady development of the flow under transonic buffet conditions 89-93